Atmos. Chem. Phys. Discuss., doi:10.5194/acp-2016-570, 2016
Manuscript under review for journal Atmos. Chem. Phys.
Published: 8 July 2016

Atmospheric Chemistry and Physics Discussions

Alteration of the microphysical properties of black carbon through transport in the boundary layer in East Asia

Takuma Miyakawa[1,2], Naga Oshima[3], Fumikazu Taketani[1,2], Yuichi Komazaki[1], Ayako Yoshino[4], Akinori Takami[4], Yutaka Kondo[5], and Yugo Kanaya[1,2]

[1]Department of Environmental Geochemical Cycle Research, Japan Agency for Marine-Earth Science and Technology, 3173-25 Showa-machi, Kanazawa-ku, Yokohama, Kanagawa, 236-0001, Japan.

[2]Institute for Arctic Climate Environment Research, Japan Agency for Marine-Earth Science and Technology, 3173-25 Showa-machi, Kanazawa-ku, Yokohama, Kanagawa, 236-0001, Japan.

[3]Meteorological Research Institute, 1-1 Nagamine, Tsukuba, Ibaraki, 305-0052, Japan

[4]Center for Regional Environmental Research, National Institute for Environmental Studies, 16-2 Onogawa, Tsukuba, Ibaraki, 305-8506, Japan

[5]National Institute for Polar Research, 10-3 Midori-cho, Tachikawa, Tokyo, 190-8518, Japan

Correspondence to: Takuma Miyakawa (miyakawat@jamstec.go.jp)

Abstract. Ground-based measurements of black carbon (BC) were performed near an industrial source region in the early summer of 2014 and at a remote island in Japan in the spring of 2015. We report the temporal variations in the transport, size distributions, and mixing states of the BC-containing particles measured using a continuous soot monitoring system, a single particle soot photometer, and an aerosol

Atmos. Chem. Phys. Discuss., doi:10.5194/acp-2016-570, 2016
Manuscript under review for journal Atmos. Chem. Phys.
Published: 8 July 2016

Atmospheric Chemistry and Physics Discussions

chemical speciation monitor. The effects of aging on the growth of BC-containing particles were examined by comparing the ground-based observations between the near-source and remote island sites. Secondary formation of sulfate aerosol through gas- and cloud-phase reactions strongly affected the increases in BC coating (i.e., enhancement of cloud condensation nuclei activity) with air mass aging from the source to the outflow regions. The effects of the wet removal on the BC microphysics were elucidated by classifying the continental outflow air masses depending on the enhancement ratio of BC to CO (ΔBC/ΔCO) ratios as an indicator of the transport efficiency of BC. It was found that ΔBC/ΔCO ratios were controlled mainly by the rainout process during transport in the planetary boundary layer (PBL) on the timescale of 1-2 days. The meteorological conditions and backward trajectory analyses suggested that air masses strongly affected by rainout originated mainly from Southern China region (20º-35ºN) during this season. Selective removal of large and thickly-coated BC-containing particles was found in air masses substantially affected by the rainout in the PBL, as predicted by Köhler theory. The size and water-solubility of BC-containing particles in the PBL can be altered by the rainout process as well as the condensation of non-BC materials.

1. Introduction

Black carbon (BC)-containing particles in atmosphere can significantly affect the radiative budget of the Earth through two effects; direct (light absorption and scattering) and indirect (aerosol-cloud interaction) effects (Bond et al., 2013; references therein). The difficulty in the estimation of these effects in the atmosphere results from both the short lifetime relative to other greenhouse gases and the variable physicochemical properties of BC-containing particles. BC itself is water-insoluble

Atmos. Chem. Phys. Discuss., doi:10.5194/acp-2016-570, 2016
Manuscript under review for journal Atmos. Chem. Phys.
Published: 8 July 2016

Atmospheric Chemistry and Physics Discussions

immediately after emission, but subsequently takes on hygroscopicity (McMeeking et al., 2011) and cloud condensation nuclei (CCN) activity (Kuwata et al., 2007) through atmospheric transport and aging. Only small amounts of water-soluble materials on BC particles are needed to cause their activation to form cloud droplets under moderate supersaturation conditions (Kuwata et al., 2007; 2009). It is considered that BC-containing particles are removed from the atmosphere mainly by the rainout process. This is because other removal processes such as gravitational settling, dry deposition, and washout cannot substantially affect the lifetime of atmospheric BC-containing particles (Seinfeld and Pandis, 2006).

The horizontal and vertical distributions of aerosols can be substantially altered by their atmospheric lifetimes (e.g., Lawrence et al., 2007). Samset et al. (2014), using multiple global model data sets constrained by aircraft observations, suggested that the atmospheric lifetime of BC largely affects its distribution, especially in the northern hemisphere, resulting in significant variations in global direct radiative forcing values. The removal of BC has been considered an important issue for the geochemical carbon cycle as well as for climate sciences. BC-containing particles deposited onto the ocean surface can affect ocean surface particles, dissolved organic carbon (DOC), and microbial processes, by absorbing DOC, stimulating particle aggregation, and changing the size distribution of suspended particles (Mari et al., 2014).

Previous modeling studies have dealt with the BC aging processes (condensational growth and coagulation) for box and regional-scale models, and parameterized timescales for conversion of BC-containing particles from water-insoluble to -soluble for global models (Oshima et al., 2009; Liu et al., 2011; Oshima and Koike, 2013). Quantitative knowledge of the variability of microphysical parameters of

Atmos. Chem. Phys. Discuss., doi:10.5194/acp-2016-570, 2016
Manuscript under review for journal Atmos. Chem. Phys.
Published: 8 July 2016

Atmospheric Chemistry and Physics Discussions

BC-containing particles and the timescale of their aging processes is still limited and is needed for near-source and remote regions (Samset et al., 2014). Moteki et al. (2012) reported the first observational evidence of the size-dependent activation of BC to form cloud droplets, in air masses uplifting from the planetary boundary layer (PBL) to the free troposphere (FT) in East Asia in the spring of 2009, during the Aerosol Radiative Forcing in East Asia (A-FORCE) aircraft campaigns (Oshima et al., 2012). The similar altitude dependence of the BC size distribution and similarity in the BC mixing state were observed in other aircraft measurements conducted in East Asia in winter (Kondo et al., 2016). Selective removal of larger BC-containing particles though the cloud process, which is predicted by Köhler theory, was qualitatively observed in the atmosphere. This observational evidence indicates that the size distributions and mixing states of BC-containing particles control the global- and regional-scale spatial distributions of BC through their upward transport from the PBL to the FT associated with rainout processes. Despite the importance of the size distributions and mixing states of BC-containing particles in the PBL, the continuous measurements of their microphysical properties are still limited around the source regions in East Asia.

Kanaya et al. (2016) have conducted long-term measurements of BC for 6 years (2009-2015) at Fukue Island, and synthetically reported the emission and removal of BC in East Asia using these data sets. It was found in their study that wet removal through transport in the PBL substantially reduced the transport efficiency of BC aerosols. Here we examine the effect of aging and wet removal during transport on the changes in BC size distributions and mixing state, as well as concentrations, based on ground-based measurements at the same site in the spring of 2015 using a single

Atmos. Chem. Phys. Discuss., doi:10.5194/acp-2016-570, 2016
Manuscript under review for journal Atmos. Chem. Phys.
Published: 8 July 2016

Atmospheric Chemistry and Physics Discussions

97 particle soot photometer (SP2) and an Aerosol Chemical Speciation Monitor (ACSM).
98 We first show the meteorological characteristics of the East Asian region in the spring
99 of 2015. Then, the loss of BC-containing particles for that period is investigated
100 using a similar approach to that used by Kanaya et al. (2016), in connection with the
101 associated changes in BC microphysics.
102
103 **2. Experimental and data analysis**
104 **2.1. Atmospheric Observations**
105 The continuous measurement of $PM_{2.5}$ and BC aerosols has been conducted at a
106 remote island, Fukue Island, since February 2009 (Kanaya et al., 2013; Ikeda et al.,
107 2014). The observation site is located at the Fukue Island Atmospheric Environment
108 Monitoring Station (32.75°N, 128.68°E, **Fig. 1**). The site is located in the northwest
109 portion of Fukue Island, approximately 20 km from the main residential area in the
110 southeast. The fine mode aerosols sampled at the site are mostly transported from
111 beyond the island. The enhanced concentrations of BC aerosol in Fukue Island are
112 mainly attributed to long-range transport from the Asian continent, according to a
113 previous study (Shiraiwa et al., 2008) and an emission inventory (**Fig. 1**, REAS ver.
114 2.1, Kurokawa et al., 2013).
115 We deployed an SP2 (Droplet Measurement Technologies, Inc., USA) for the
116 analysis of microphysical parameters of refractory BC (rBC, Petzold et al., 2013) from
117 March 26, 2015 to April 14, 2015. The SP2 was calibrated before starting the
118 ambient measurements. The calibration protocol for our SP2 is described in
119 Miyakawa et al. (2016). Mass equivalent diameter (MED) was derived from the rBC
120 mass per particle (m_{pp}) with the assumed particle density of BC (1800 kg m^{-3}, Bond
121 and Bergstrom, 2006). A large diameter Nafion dryer (MD-700, Perma Pure, Inc.,

Atmos. Chem. Phys. Discuss., doi:10.5194/acp-2016-570, 2016
Manuscript under review for journal Atmos. Chem. Phys.
Published: 8 July 2016

Atmospheric Chemistry and Physics Discussions

122 USA) was placed in front of the SP2 for drying the sample air without significant loss
123 of the aerosol particles greater than 50 nm. The dry air for MD-700 was generated by
124 a heatless dryer (HD-2000, Perma Pure, Inc., USA) and a compressor
125 (2AH-23-M222X, MFG Corp., USA). The relative humidity of the sample air was
126 less than 20% during the observation period. The hourly number/mass size
127 distributions and hourly median values of shell (D_S) to rBC diameter (D_{core}) ratio
128 (D_S/D_{core}) for the selected D_{core} ranges were calculated. The retrieval of D_S from the
129 light scattering signals measured by an avalanche photodiode and a position sensitive
130 detector (Gao et al., 2007) were performed using a time-resolved scattering cross
131 section method given by Laborde et al. (2012). We also analyzed the microphysical
132 parameters of rBC particles measured using the SP2 in the early summer of 2014 at
133 Yokosuka (35.32°N, 139.65°E, **Fig. 1**), located near industrial sources beside Tokyo
134 Bay (Miyakawa et al., 2016). These data sets were used as a reference for the
135 BC-containing particles in air masses strongly affected by combustion sources.
136 Equivalent BC (EBC, Petzold et al., 2013) mass concentrations are continuously
137 measured at Fukue Island using two instruments; a continuous soot-monitoring system
138 (COSMOS; model 3130, Kanomax, Japan), and a multi-angle absorption photometer
139 (MAAP; MAAP5012, Thermo Scientific, Inc., USA). The details of the air sampling
140 and intercomparison for EBC measurements at Fukue Island have been described
141 elsewhere (Kanaya et al., 2013; 2016). In this study, mass concentrations of EBC
142 measured using the COSMOS were evaluated by comparison with those of
143 SP2-derived rBC. The intercomparison between SP2 and COSMOS will be briefly
144 discussed in the following.
145 **Figure 2** depicts the correlation between COSMOS-EBC and SP2-rBC hourly mass

Atmos. Chem. Phys. Discuss., doi:10.5194/acp-2016-570, 2016
Manuscript under review for journal Atmos. Chem. Phys.
Published: 8 July 2016

Atmospheric Chemistry and Physics Discussions

concentrations. The unmeasured fraction of the rBC mass was corrected by extrapolation of the lognormal fit for the measured mass size distributions, to the outsides of the lower and upper boundaries (0.08 and 0.5 μm, respectively). Note that the uncertainty with respect to the unmeasured fraction of rBC mass was minor (<5%) in this study. The linear regression slope of the correlation between EBC and rBC was 0.88 (±0.03). Uncertainty with respect to the calibration was examined in an industrial region and found to be within around 3% (Miyakawa et al., 2016). The average discrepancy between EBC and rBC was beyond the uncertainty of the calibration and was comparable to the uncertainty of COSMOS (10%) as evaluated by Kondo et al. (2009). Onsite calibration of the SP2 using ambient BC particles prepared by thermal denuder and particle mass classifier, such as an aerosol particle mass analyzer (APM), is desirable for the better quantification of rBC mass based on the laser-induced incandescence technique in a remote area. Although we need further attempts to evaluate SP2 in remote area, this study suggested that SP2-rBC mass concentrations agreed well with COSMOS-EBC within the uncertainty of COSMOS. Therefore we simply use "BC", instead of EBC and rBC defined depending upon the measurement techniques. We analyzed the COSMOS data for the BC mass concentration, and the SP2 data for the BC microphysics.

The chemical composition of non-refractory submicron aerosols was measured using an Aerodyne Aerosol Chemical Speciation Monitor (ACSM, Aerodyne, Inc., USA.) placed in an observatory container at Fukue Island during the observation period. The details of the ACSM at Fukue Island have been described in Irei et al. (2014). The collection efficiency (CE) of the ACSM was assumed to be 0.5 for this period. We considered sulfate (SO_4^{2-}) ion as a major non-BC material and the most

Atmos. Chem. Phys. Discuss., doi:10.5194/acp-2016-570, 2016
Manuscript under review for journal Atmos. Chem. Phys.
Published: 8 July 2016

Atmospheric Chemistry and Physics Discussions

important secondary aerosol in East Asia (Takami et al., 2007) for the data interpretation. During the period April 1 -7, 2015, the critical orifice of the inlet assembly of the ACSM was clogged. ACSM-derived SO_4^{2-} (ACSM- SO_4^{2-}) for this period is not used in the analysis.

Two high volume air samplers (HV500F, Sibata Scientific Technology, Ltd., Japan) were deployed on the rooftop of the observatory container. The sampling flow rate for both samplers was 500 liters per minute (lpm). Air sampling was carried out for 21 h (from 10:00 AM to 7:00 AM) on a 110-mm pre-combusted (900°C for 3 h) quartz filter (QR-100, Advantec Toyo Kaisha Ltd., Japan). Both have a $PM_{2.5}$ impactor for classifying the particle size. One impaction plate was coated with vacuum grease (HIVAC-G, Shin-Etsu Chemical Co., Ltd., Japan) to minimize the impact of coarse mode particles on the chemical analysis of fine mode particles such as radiocarbon analysis, and a pre-combusted quartz fiber filter with slits was set on another impaction plate to collect coarse particles. Water soluble ions were analyzed using ion chromatography (Dionex ICS1000, Thermo Fisher Scientific K.K., Japan). The results from the chemical analysis of filter samples are not included in this study in detail. We only used the mass concentration of sulfate ion (IC-SO_4^{2-}) in this study to evaluate the uncertainty in relation to CE of the ACSM, and to analyze the temporal variations during the period when the ACSM-SO_4^{2-} data are not available (April 1-7, 2015).

The carbon monoxide (CO) mixing ratio is also continuously measured using a nondispersive infrared (NDIR) CO monitor (model 48C, Thermo Scientific, Inc. USA). Details of CO measurements including the long-term variations in sensitivity and zero level are discussed elsewhere (Kanaya et al., 2016).

Atmos. Chem. Phys. Discuss., doi:10.5194/acp-2016-570, 2016
Manuscript under review for journal Atmos. Chem. Phys.
Published: 8 July 2016

Atmospheric Chemistry and Physics Discussions

194

195 **2.2. Enhancement ratio of BC to CO as an indicator of the BC removal**

196 In order to quantify the extent of the removal of BC, we calculated the enhancement
197 ratio of BC mass concentrations to CO mixing ratios (ΔBC/ΔCO) against the East
198 Asian background air concentrations as follows:

199

200 $$\frac{\Delta BC}{\Delta CO} = \frac{[BC] - [BC]_{bg}}{[CO] - [CO]_{bg}}, \quad (1)$$

201

202 where [BC] and [CO] are measured concentrations of the BC and CO respectively, and
203 $[BC]_{bg}$ and $[CO]_{bg}$ are their background concentrations. Here we assumed that $[BC]_{bg}$
204 is zero (Oshima et al., 2012). The background concentration of CO during the period
205 (March 11 – April 14, 2015) was calculated by averaging the concentrations lower than
206 the 5th percentile (120 ppb).

207

208 **2.3. Meteorological field analysis**

209 We used 6-hourly meteorological data, with a resolution of 1° in latitude and
210 longitude, from the National Centers for Environmental Prediction (NCEP) Final
211 (FNL) operational global analysis; and daily precipitation data, with a resolution of 1°
212 in latitude and longitude, from the Global Precipitation Climatology Project (GPCP)
213 data set (Huffman et al., 2001). We analyzed these data sets to investigate the general
214 features of the meteorological field in East Asia during the observation period.

215

Atmos. Chem. Phys. Discuss., doi:10.5194/acp-2016-570, 2016
Manuscript under review for journal Atmos. Chem. Phys.
Published: 8 July 2016

Atmospheric Chemistry and Physics Discussions

2.4. Backward trajectory analysis

We calculated backward trajectories from the observation site to elucidate the impact of the Asian outflow. 3-day backward trajectories from the observation site (the starting altitude was 0.5 km) were calculated every hour using the NOAA Hybrid Single-Particle Lagrangian Integrated Trajectory model (Draxler and Rolph, 2012; Rolph, 2012) with the meteorological data sets (NCEP's GDAS). In this study, the residence time over specific source regions was used as an indicator of their impacts on the observed air masses. We defined five domains for assessing the impact over the Asian continent; Northeast China (NE), Korea (KR), Central North China (CN), Central South China (CS), and Japan (JP) (**Fig. 1**). The period when air masses passed over the domains NE, KR, CN, and CS at least for one hour is defined as that of "continental outflow". The impacts of precipitation on the observed air masses were assessed by a parameter "Accumulated Precipitation along Trajectory" (APT, Oshima et al., 2012). In this study, we calculated the APT values by integrating the amount of hourly precipitation in the Lagrangian sense along each 3-day back trajectory of the sampled air masses. The hourly variations of APT were merged into the observed gas and aerosol data sets.

3. Results and discussion

3.1. The meteorological field in the spring of 2015

The mean meteorological field during the observation period (March 11–April 14, 2015) is discussed for the purpose of characterizing the general features of the wind flow and precipitation in this region. **Figure 3a** shows the mean sea level pressure (SLP) and mean horizontal winds at the 850 hPa level in East Asia during the observation period. The mean equivalent potential temperature (θe) and the

Atmos. Chem. Phys. Discuss., doi:10.5194/acp-2016-570, 2016
Manuscript under review for journal Atmos. Chem. Phys.
Published: 8 July 2016

Atmospheric Chemistry and Physics Discussions

meridional moisture transport at the 850 hPa level during the same period are also shown in **Figure 3b**. The mid-latitude region (35-50°N, 120-140°E) was under the influence of a modest monsoonal northwesterly flow, which advected cold, dry air from the continent to the observation area. The subtropical region (20°-30°N, 110°-130°E) was under the influence of a persistent southwesterly flow, part of which was conversing into the observation area (30°-35°N), being confluent with the northwesterlies from the continent. The low-level southerly flow advected warm, moist air into the observation area to sustain a large amount of precipitation (**Fig. 4a**).

Figure 3c shows the temporal variations in surface pressure and precipitable water at the observation site. The surface pressure is well anti-correlated with the precipitable water. During the observation period, migratory cyclones and anticyclones occurred occasionally (3 times each). The occurrence of migratory cyclones advected moist air, which could contribute to the wet removal of BC during transport in the PBL. In contrast, the occurrence of anticyclones advected dry air, which could contribute to the efficient transport of BC from the source regions.

Figure 4a depicts the mean precipitation over East Asia during the observation period. Mean precipitation showed a latitudinal gradient over eastern China and the Yellow Sea and East China Sea region (i.e., increasing precipitation from South to North), suggesting that transport pathways can greatly affect the wet removal of aerosols. The APT was compared with the averaged latitude of each trajectory for 48 h backwardly from the time of -24 h (Lat_{ORIG}) (**Fig. 4b**), which can be interpreted as an indicator for the latitudinal origin of air masses arriving at Fukue Island. The high APT values corresponded to air masses originated from southern regions (20º-40ºN). The data points are colored according to the maximum RH values along each

Atmos. Chem. Phys. Discuss., doi:10.5194/acp-2016-570, 2016
Manuscript under review for journal Atmos. Chem. Phys.
Published: 8 July 2016

Atmospheric Chemistry and Physics Discussions

backward trajectory (RH_{max}). The lower RH_{max} were observed in the air masses with low APT values and originated from northern regions (30º-50ºN). These air mass characteristics are consistent with the mean precipitation field (**Fig. 4a**). Some of the data points showed high values of RH_{max} (~100%) when their APT was almost zero. These data would correspond to the air masses that experienced cloud process not associated with precipitation. Possible effects of cloud process without precipitation on the removal of aerosol particles during transport will be discussed using these data points in the following section.

3.2. Temporal variations in BC, SO_4^{2-}, and CO

Temporal variations in concentrations of BC (measured using COSMOS and SP2), SO_4^{2-} (measured using ACSM and IC), and CO are shown in **Figure 5** (middle and bottom panels respectively). ACSM-SO_4^{2-} generally agreed well with IC-SO4, indicating that the assumed CE (0.5) was valid for the observation period. In general, BC and SO_4^{2-} were positively correlated with CO at Fukue Island, showing the impact of continental outflow affected by incomplete combustion sources for aerosol mass concentrations. **Figure 5** also includes the temporal variation in the fractional residence time over the selected region defined in section 2.4 (top panel). The CO concentrations were typically enhanced for the period with the higher contributions of CN and CS. The positive correlation of SO_4^{2-} and CO suggests that the secondary formation of SO_4^{2-} through transport was significant during the observation period, and that SO_4^{2-} contributed to the coating of BC-containing particles. A previous study suggested that the majority of SO_4^{2-} aerosol was formed by less than around 1.5 days after the air masses left the Chinese continent (Sahu et al., 2009). Kanaya et al.

Atmos. Chem. Phys. Discuss., doi:10.5194/acp-2016-570, 2016
Manuscript under review for journal Atmos. Chem. Phys.
Published: 8 July 2016

289 (2016) showed that the typical transport time of continental outflow air masses at
290 Fukue Island was around 1-2 days in spring. The small variability of SO_4^{2-}/CO ratios
291 is consistent with these facts. The period with the APT > 3 mm is highlighted by light
292 blue in **Figure 5** to show the impact of wet removal on the transport of BC and SO_4^{2-}
293 aerosols. The maximum concentrations of BC, SO_4^{2-}, and CO were observed on the
294 morning of March 22 (Ep.1) under the influence of the anticyclone (corresponding to
295 the trajectories colored red in **Fig. 4a**) when the APT values were almost zero. In
296 contrast, BC and SO_4^{2-} concentrations did not increase with CO in the period from the
297 evening of April 5 to the morning of April 6 (Ep.2) under the influence of the
298 migratory cyclone (corresponding to the trajectories colored black in **Fig. 4a**), when
299 the APT was greater than 10 mm.
300
301 **3.3. Correlation of BC, SO_4^{2-}, and CO as an indicator of the removal of aerosols**
302 **Figures 6a** and **6b** show scatter plots of CO with BC and SO_4^{2-}, respectively.
303 Positive correlation of BC and SO_4^{2-} with CO was clearly found in air masses with low
304 APT values. It is evident from these scatter plots that the correlations of BC/CO and
305 SO_4^{2-}/CO are mainly affected by APT. The cloud process of aerosol particles not
306 associated with precipitation can also reduce the slope of their correlation. However,
307 no decreasing tendency of BC/CO and SO_4^{2-}/CO against RH_{max} when APT was zero
308 was found during the observation period (not shown). Kanaya et al. (2016) found that
309 the estimated emission ratios of BC to CO over the East Asian continent ranged from
310 5.3 (±2.1) to 6.9 (±1.2) ng m^{-3} ppb^{-1}, slightly depending on the origin of the air masses
311 (this range is overlaid on **Fig. 6a**). ΔBC/ΔCO observed in the PBL over the Yellow
312 Sea in the same season was 6.2 ng m^{-3} ppb^{-1} (Kondo et al., 2016). The data points

Atmos. Chem. Phys. Discuss., doi:10.5194/acp-2016-570, 2016
Manuscript under review for journal Atmos. Chem. Phys.
Published: 8 July 2016

313 with ΔBC/ΔCO in these ranges show low APT values (less than or ~1 mm). Wet
314 removal (rainout) was one of the most important controlling factors on the transport
315 efficiency of BC in this region during the observation period. The use of the
316 ΔBC/ΔCO ratios is feasible for examining the wet removal of BC during the
317 observation period. The SO_4^{2-}/CO slope slightly increased with RH_{max} increasing
318 when the APT was zero, as indicated in the subset of **Figure 6b**, suggesting that
319 aqueous phase formation and subsequent droplet evaporation partly contributed to the
320 mass concentrations of SO_4^{2-} observed at Fukue Island. Therefore, the changes in the
321 SO_4^{2-}/CO correlation are controlled largely by the rainout process and weakly by
322 aqueous-phase formation during transport.
323
324 **3.4. Changes in microphysical parameters of BC-containing particles associated**
325 **with wet removal**
326 Number- and mass-size distributions of BC classified by the values of ΔBC/ΔCO are
327 shown in **Figures 7a** and **7b**, respectively. When ΔBC/ΔCO values in continental
328 outflow air masses are greater than 3 ng m^{-3} ppb^{-1} (within the range of the BC/CO
329 emission ratios given by Kanaya et al. 2016), these air masses are defined as "outflow
330 without BC loss". These air masses originated mainly from CN via KR and NE.
331 When ΔBC/ΔCO values of continental outflow air masses are less than 1 ng m^{-3} ppb^{-1},
332 the air masses are defined as "outflow with BC loss". Considering the typical
333 emission ratios of BC to CO (6-7 ng m^{-3} ppb^{-1}; Kanaya et al., 2016), transport
334 efficiency for the "outflow with BC loss" air masses can be estimated to be less than
335 ~17%. These air masses originated mainly in CS. The low and high APT values for
336 "outflow without BC loss" and "outflow with BC loss" air masses, respectively, give
337 confidence in the validity of our classification as discussed in the previous section.

Atmos. Chem. Phys. Discuss., doi:10.5194/acp-2016-570, 2016
Manuscript under review for journal Atmos. Chem. Phys.
Published: 8 July 2016

As a reference for emission sources ("source"), the average size distributions of BC in a Japanese industrial area (see section 2.1, Miyakawa et al., 2016) are shown in **Figure 7**. The statistics of the size distributions were summarized in **Table 1**. Observed differences in the size distributions between source and outflow were generally consistent with previous studies (Schwarz et al., 2010). Air mass aging leads to the growth of BC-containing particles. Number-size distributions of BC largely varied in the size range less than 0.1 μm (**Fig. 7a**). In outflow air masses, such small BC-containing particles were scavenged by larger particles in the coagulation process during transport. The peak diameter of mass (number) size distributions of BC became larger, from 0.16 (0.06) μm to 0.18-0.2 (0.09-0.1) μm, between source and outflow. BC-containing particles have systematically different size distributions in outflow air masses with and without BC loss, indicating that the BC loss process also affected the size distributions. The peak diameter of BC number and mass size distributions in outflow air masses with BC loss was slightly lower than without BC loss.

Figure 8 depicts the probability density of the D_S/D_{core} ratio for the BC size of 0.2 (±0.02) μm, for source and outflow air masses. The modal values of the D_S/D_{core} ratio were systematically changed with air mass aging and BC loss (wet removal). The condensation of inorganic and organic vapors on BC-containing particles during transport can account for the increase in the D_S/D_{core} ratio, as discussed in previous studies (e.g., Subramanian et al. 2010; Shiraiwa et al., 2008). As discussed earlier, this study suggested that SO_4^{2-} substantially contributed the increase in the D_S/D_{core} ratio. In outflow air masses with BC loss, modal values of the D_S/D_{core} ratio were clearly lower than in outflow without BC loss. It is indicated that the wet removal

Atmos. Chem. Phys. Discuss., doi:10.5194/acp-2016-570, 2016
Manuscript under review for journal Atmos. Chem. Phys.
Published: 8 July 2016

Atmospheric Chemistry and Physics Discussions

process also affected the coating thickness distributions for the BC sizes in the range 0.15-0.35 μm (**Table 1**). It should be noted that the coating of BC-containing particles is not always thick in remote regions, and that the D_S/D_{core} ratio distributions, as well as size distributions, can be affected by the wet removal process during transport in the PBL.

3.5. Discussion

Not only in-cloud scavenging of BC-containing particles but also subsequent precipitation (i.e., rainout process) can account for the changes in the microphysical parameters of BC detected in this study. Our results show the decrease of both the peak diameter of the BC mass size distribution, and the modal value of the D_S/D_{core} ratios in relation to the rainout. The observed evidence implies the selective removal of large and water-soluble BC-containing particles during transport in the PBL. The Köhler theory suggests that a lower super saturation is needed for the large and highly water-soluble particles, and qualitatively accounts for the observed changes in the BC microphysics.

Note that the magnitude of the change in the BC size distributions in the PBL (0.01-0.02 μm (~1 fg)) shown in this study is smaller than that observed in air masses uplifted from the PBL to the FT, associated with wet removal (~0.04 μm (~3 fg), Fig 2 of Moteki et al., 2012) at a similar level of transport efficiency (<~20%). Air masses sampled at the ground level would be affected by turbulent mixing of those near the cloud around the top of the PBL and those in cloud-free conditions at below-cloud. On the other hands, most air masses sampled by the aircraft measurements in the FT would experience the cloud process during upward transport from the PBL. Mixing

Atmos. Chem. Phys. Discuss., doi:10.5194/acp-2016-570, 2016
Manuscript under review for journal Atmos. Chem. Phys.
Published: 8 July 2016

386 of air masses in the PBL suggests their partial experience of the in-cloud scavenging
387 processes and therefore the suppression of the changes in the microphysical properties
388 of BC-containing particles during transport in the PBL. The transport pathways of
389 the continental outflow air masses are horizontally and vertically variable in spring in
390 East Asia because of the frequent alternative cyclone/anticyclone activities in spring
391 (Asai et al., 1988). Oshima et al. (2013) have examined the three-dimensional
392 transport pathways of BC over East Asia in spring and showed that the PBL outflow
393 through which BC originating from China was advected by the low-level westerlies
394 without uplifting out of the PBL was one of the most major pathways for BC export
395 from continental East Asia to the Pacific, supporting the general features of
396 microphysical properties of BC in continental outflow obtained by this study. Mori et
397 al. (2014) measured the seasonal variations in BC wet deposition fluxes at another
398 remote island in Japan (Okinawa, ~500 km south of Fukue Island), and revealed their
399 maxima in spring, which is consistent with the seasonal variations in the cyclone
400 frequencies. It is suggested that BC-containing particles were efficiently activated to
401 form cloud droplets in the continental outflow air masses, and can affect the cloud
402 physicochemical properties in spring in East Asia, as indicated by Koike et al. (2012).
403 To further understand the possible connections of the variabilities in BC microphysical
404 properties and meteorological conditions in this region can provide useful constraints
405 on the better prediction of climatic impacts of BC-containing particles (Matsui, 2016).
406
407 **4. Conclusions**
408 Ground-based measurements of BC were performed near an industrial source region
409 and at a remote island in Japan. We have reported the temporal variations in the

Atmos. Chem. Phys. Discuss., doi:10.5194/acp-2016-570, 2016
Manuscript under review for journal Atmos. Chem. Phys.
Published: 8 July 2016

Atmospheric Chemistry and Physics Discussions

410 transport and the microphysics of the BC-containing particles, measured using the
411 COSMOS, SP2, and ACSM. The impacts of air mass aging upon the growth of
412 BC-containing particles were examined by comparing the ground-based observations
413 between the near-source and remote island sites. ΔBC/ΔCO was used as an indicator
414 of the transport efficiency of BC, because it was controlled mainly by rainout during
415 transport in the PBL. The BC size and coating increased during transport from the
416 near-source to the outflow regions on the timescale of 1-2 days when the rainout
417 during transport was negligible. SO_4^{2-} aerosol was secondarily formed both in gas-
418 and cloud-phase during transport, and contributed to the significant increase in the
419 coating materials of BC (i.e., enhanced whole size and water-solubility of
420 BC-containing particles). Decreases in the peak diameter of mass size distributions
421 (~0.01 μm) and modal D_S/D_{core} ratios (~0.4 for BC of 0.2 μm) of BC-containing
422 particles were observed in air masses substantially affected by rainout. The observed
423 evidences, selective removal of large and water-soluble BC-containing particles, are
424 qualitatively consistent with the Köhler theory; however they are not as large as those
425 found in air masses uplifted from the PBL to the FT in East Asia associated with
426 precipitation. The mixing of below-cloud and in-cloud air masses in the PBL would
427 result in suppression of the degree of changes in BC microphysical parameters by
428 cloud processes. This study indicates (1) that the changes (sign and degree) in BC
429 microphysics can be affected by how the air masses are transported, (2) that the
430 observed selective removal of large and water-soluble BC-containing particles in East
431 Asia are expected to be significant in the PBL as well as the FT in East Asia.
432
433

Atmos. Chem. Phys. Discuss., doi:10.5194/acp-2016-570, 2016
Manuscript under review for journal Atmos. Chem. Phys.
Published: 8 July 2016

Atmospheric Chemistry and Physics Discussions

Acknowledgments

This study was supported by the Environment Research and Technology Development Fund (S7, S12, and 2-1403) of the Ministry of Environment, Japan, the Japan Society for the Promotion of Science (JSPS), KAKENHI Grant numbers 26550021, 26701004, 26241003, and 16H01770, and partially carried out in the Arctic Challenge for Sustainability (ArCS) Project. The authors would like to thank N. Moteki at the University of Tokyo for assistance with the SP2 calibrations. M. Kubo, T. Takamura, and H. Irie (Chiba University) are also acknowledged for their support at the Fukue-Island Atmospheric Environment Monitoring Station.

References

Asai, T., Y. Kodama, and J.-C. Zhu, Long-term variations of cyclone activities in East Asia, Adv. Atmos. Sci., 5, 149−158, 1988.

Bond, T. C. and R. W. Bergstrom, Light Absorption by Carbonaceous Particles: An Investigative Review, Aerosol Sci. Technol., 40, 27-67, 2006.

Bond, T., et al.. Bounding the role of black carbon in the climate system: a scientific assessment. J. Geophys. Res., 118, 5380–5552, doi:10.1002/jgrd.50171, 2013.

Draxler, R. R., and Rolph, G. D., HYSPLIT (HYbrid Single-Particle Lagrangian Integrated Trajectory) Model access via NOAA ARL READY Website (http://ready.arl.noaa.gov/ HYSPLIT.php), NOAA Air Resources Laboratory, Silver Spring, Md., 2012

Gao, R. S., Schwarz, J. P., Kelly, K. K., Fahey, D. W., Watts, L. A., Thompson, T. L., Spackman, J. R., Slowik, J. G., Cross, E. S., Han, J. H., Davidovits, P., Onasch, T. B., and Worsnop, D. R., A novel method for estimating light-scattering properties of soot aerosols using a modified single-particle soot photometer, Aerosol Sci.

459 Tech., 41, 125–135, 2007
460 Hinds, W. C., Aerosol Technology: Properties, Behavior, and Measurement of Airborne
461 Particles, Wiley-Interscience, New York, 1999
462 Huffman, G.J., R.F. Adler, M. Morrissey, D.T. Bolvin, S. Curtis, R. Joyce, B
463 McGavock, and J. Susskind, Global Precipitation at One-Degree Daily Resolution
464 from Multi-Satellite Observations. *J. Hydrometeor*., 2, 36-50, 2001
465 Ikeda, K., K. Yamaji, Y. Kanaya, F. Taketani, X. Pan, Y. Komazaki, J. Kurokawa, and T.
466 Ohara, Sensitivity Analysis of Source Regions to PM2.5 Concentration at Fukue
467 Island, Japan, J. Air Waste Manage. Assoc., doi:10.1080/10962247.2013.845618,
468 2014
469 Irei, S., A. Takami, M. Hayashi, Y. Sadanaga, K. Hara, N. Kaneyasu, K. Sato, T.
470 Arakaki, S. Hatakeyama, H. Bandow, T. Hikida, and A. Shimono, Transboundary
471 Secondary Organic Aerosol in Western Japan Indicated by the δ13C of
472 Water-Soluble Organic Carbon and the m/z 44 Signal in Organic Aerosol Mass
473 Spectra, Environ. Sci. Technol., 48, 6273-6281, 2014
474 Kanaya, Y., F. Taketani, Y. Komazaki, X. Liu, Y. Kondo, L. K. Sahu, H. Irie, and H.
475 Takashima, Comparison of black carbon mass concentrations observed by
476 Multi-Angle Absorption Photometer (MAAP) and Continuous Soot-Monitoring
477 System (COSMOS) on Fukue Island and in Tokyo, Japan, Aerosol Sci. Technol.,
478 47, 1-10, 2013
479 Kanaya, Y., X. Pan, T. Miyakawa, Y. Komazaki, F. Taketani, I. Uno, and Y. Kondo,
480 Long-term observations of black carbon mass concentrations at Fukue Island,
481 western Japan, during 2009-2015: Constraining wet removal rates and emission
482 strengths from East Asia, Atmos. Phys. Chem. Discuss., doi:10.5194/acp-2016-213,

2016

Koike, M., N. Takegawa, N. Moteki, Y. Kondo, H. Nakamura, K. Kita, H. Matsui, N. Oshima, M. Kajino, and T. Y. Nakajima, Measurements of regional-scale aerosol impacts on cloud microphysics over the East China Sea: Possible influences of warm sea surface temperature over the Kuroshio ocean current, J. Geophys. Res., 117, D17205, doi:10.1029/2011JD017324, 2012

Kondo, Y., L. Sahu, N. Moteki, F. Khan, N. Takegawa, X. Liu, M. Koike and T. Miyakawa, Consistency and Traceability of Black Carbon Measurements Made by Laser-Induced Incandescence, Thermal-Optical Transmittance, and Filter-Based Photo-Absorption Techniques, Aerosol Sci. Technol., 45, 295-312, 2009

Kondo, Y., N. Moteki, N. Oshima, S. Ohata, M. Koike, Y. Shibano, N. Takegawa, and K. Kita, Effects of Wet Deposition on the Abundance and Size Distribution of Black Carbon in East Asia, J. Geophys. Res. Atmos., 121, doi:10.1002/2015JD024479, 2016

Kurokawa, J., T. Ohara, T. Morikawa, S. Hanayama, G. Janssens-Maenhout, T. Fukui, K. Kawashima, and H. Akimoto, Emissions of air pollutants and greenhouse gases over Asian regions during 2000-2008: Regional Emission inventory in ASia (REAS) version 2, Atmos. Chem. Phys., 13, 11019-11058, doi:10.5194/acp-13-11019-2013, 2013

Kuwata, M., Y. Kondo, M. Mochida, N. Takegawa, and K. Kawamura, Dependence of CCN activity of less volatile particles on the amount of coating observed in Tokyo, J. Geophys. Res., 112, D11207, doi:10.1029/2006JD007758, 2007

Kuwata, M., Y. Kondo, and N. Takegawa, Critical condensed mass for activation of black carbon as cloud condensation nuclei in Tokyo, J. Geophys. Res., 114,

D20202, doi:10.1029/2009JD012086, 2009

Laborde, M., Mertes, P., Zieger, P., Dommen, J., Baltensperger, U., and Gysel, M., Sensitivity of the Single Particle Soot Photometer to different black carbon types, Atmos. Meas. Tech., 5, 1031–1043, doi:10.5194/amt-5-1031-2012, 2012

Lawrence, M., T. M. Butler, J. Steinkamp, B. R. Gurjar, and J. Lelieveld, Regional pollution potentials of megacities and other major population centers, Atmos. Chem. Phys., 7, 3969-3987, 2007

Liu, J., S. Fan, L. W. Horowitz, and H. Levy II, Evaluation of factors controlling long-range transport of black carbon to the Arctic, J. Geophys. Res., 116, D04307, doi:10.1029/2010JD015145, 2011

Mari, X., et al., Effects of soot deposition on particle dynamics and microbial processes in marine surface waters, Global Biogeochem. Cycles, 28, 662–678, doi:10.1002/2014GB004878, 2014

Matsui, H., Black carbon simulations using a size- and mixing-state-resolved three-dimensional model: 1. Radiative effects and their uncertainties, J. Geophys. Res. Atmos., 121, 1793–1807, doi:10.1002/2015JD023998, 2016

McMeeking, G. R., N. Good, M. D. Petters, G. McFiggans, and H. Coe, Influences on the fraction of hydrophobic and hydrophilic black carbon in the atmosphere, Atmos. Chem. Phys., 11, 5099-5112, 2011

Miyakawa, T., Y. Kanaya, Y. Komazaki, F. Taketani, X. Pan, M. Irwin, J. Symonds, Intercomparison between a single particle soot photometer and evolved gas analysis in an industrial area in Japan: Implications for the consistency of soot aerosol mass concentration measurements, Atmos. Environ., 127, 14-21, 2016

Mori, T., Y. Kondo, S. Ohata, N. Moteki, H. Matsui, N. Oshima, and A. Iwasaki, Wet

531 deposition of black carbon at a remote site in the East China Sea, J. Geophys. Res.
532 Atmos., 119, 10,485–10,498, doi:10.1002/2014JD022103, 2014
533 Moteki, N., Y. Kondo, N. Oshima, N. Takegawa, M. Koike, K. Kita, H. Matsui, and M.
534 Kajino, Size dependence of wet removal of black carbon aerosols during transport
535 from the boundary layer to the free troposphere, Geophys. Res. Lett., 39, L13802,
536 doi:10.1029/2012GL052034, 2012
537 Oshima, N., M. Koike, Y. Zhang, Y. Kondo, N. Moteki, N. Takegawa, and Y.
538 Miyazaki, Aging of black carbon in outflow from anthropogenic sources using a
539 mixing state resolved model: Model development and evaluation, J. Geophys. Res.,
540 114, D06210, doi:10.1029/2008JD010680, 2009
541 Oshima, N., et al., Wet removal of black carbon in Asian outflow: Aerosol Radiative
542 Forcing in East Asia (A-FORCE) aircraft campaign, J. Geophys. Res., 117,
543 D03204, doi:10.1029/2011JD016552, 2012
544 Oshima, N., and M. Koike, Development of a parameterization of black carbon aging
545 for use in general circulation models, Geophys. Model. Dev., 6, 263-282, 2013
546 Oshima, N., M. Koike, Y. Kondo, H. Nakamura, N. Moteki, H. Matsui, N. Takegawa,
547 and K. Kita, Vertical transport mechanisms of black carbon over East Asia in
548 spring during the A-FORCE aircraft campaign, J. Geophys. Res. Atmos., 118,
549 13,175–13,198, doi:10.1002/2013JD020262, 2013
550 Petzold, A., J.A. Ogren, M., Fiebig, S. M. Li, U. Bartensperger, T. Holzer-Popp, S.
551 Kinne, G. Pappalardo, N. Sugimoto, C. Wehrli, A. Wiedensohler, and X. Y. Zhang,
552 Recommendations for reporting “black carbon” measurements, Atmos. Chem.
553 Phys. 13, 8365-8379, 2013
554 Rolph, G. D., Real-time Environmental Applications and Display system (READY)

Atmos. Chem. Phys. Discuss., doi:10.5194/acp-2016-570, 2016
Manuscript under review for journal Atmos. Chem. Phys.
Published: 8 July 2016

555 Website (http://ready.arl.noaa.gov). NOAA Air Resources Laboratory, Silver
556 Spring, Md., 2002
557 Sahu, L. K., Y. Kondo, Y. Miyazaki, M. Kuwata, M. Koike, N. Takegawa, H.
558 Tanimoto, H. Matsueda, S. C. Yoon, and Y. J. Kim, Anthropogenic aerosols
559 observed in Asian continental outflow at Jeju Island, Korea, in spring 2005, J.
560 Geophys. Res., 114, D03301, doi:10.1029/2008JD010306, 2009
561 Samset, B. H., et al., Modelled black carbon radiative forcing and atmospheric lifetime
562 in AeroCom Phase II constrained by aircraft observations, Atmos. Phys. Chem., 14,
563 12465-12477, 2014
564 Schwarz, J. P., J. R. Spackman, R. S. Gao, L. A. Watts, P. Stier, M. Schulz, S. M.
565 Davis, S. C. Wofsy, and D. W. Fahey, Global‐scale black carbon profiles
566 observed in the remote atmosphere and compared to models, Geophys. Res. Lett.,
567 37, L18812, doi:10.1029/2010GL044372, 2010
568 Seinfeld, J.H., and Pandis, S. N., Atmospheric Chemistry and Physics, 2nd ed., John
569 Wiley &Sons, New York, 2006
570 Shiraiwa M., Y. Kondo, N. Moteki, N. Takegawa, L. K. Sahu, A. Takami, S.
571 Hatakeyama, S. Yonemura, D. R. Blake, Radiative impact of mixing state of black
572 carbon aerosol in Asian outflow, J. Geophys. Res. 113, D24210,
573 doi:10.1029/2008JD010546, 2008
574 Subramanian, R., G. L. Kok, D. Baumgardner, A. Clarke, Y. Shinozuka, T. L. Campos,
575 C. G. Heizer, B. B. Stephens, B. de Foy, P. B. Voss, and R. A. Zaveri, Black
576 carbon over Mexico: the effect of atmospheric transport on mixing state, mass
577 absorption cross-section, and BC/CO ratios, Atmos. Chem. Phys., 10, 219-237,
578 2010

Atmos. Chem. Phys. Discuss., doi:10.5194/acp-2016-570, 2016
Manuscript under review for journal Atmos. Chem. Phys.
Published: 8 July 2016

579 Takami A., T. Miyoshi, A. Shimono , N. Kaneyasu , S. Kato, Y. Kajii, S. Hatakeyama,
580 Transport of anthropogenic aerosols from Asia and subsequent chemical
581 transformation. J. Geophys. Res., 112 (D22S31), doi:10.1029/2006JD008120, 2007
582

Atmos. Chem. Phys. Discuss., doi:10.5194/acp-2016-570, 2016
Manuscript under review for journal Atmos. Chem. Phys.
Published: 8 July 2016

Atmospheric Chemistry and Physics Discussions

583 **Figures**

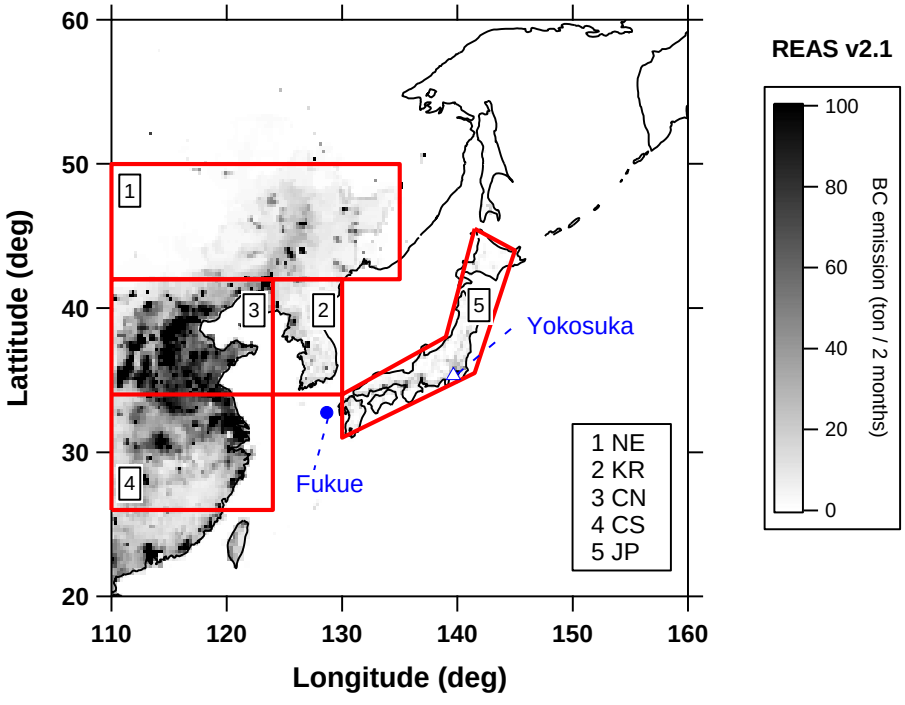

584

585

586 **Figure 1.** Map of the investigated region with two observation sites (Yokosuka, open
587 triangle; Fukue Island, closed circle) and five defined areas (1 Northeast China; 2
588 Korea; 3 Central North China; 4 Central South China; 5 Japan). The bimonthly mean
589 BC emission rate (March-April) in 2008 is overlaid on the map (REAS ver. 2.1,
590 Kurokawa et al., 2013).

591

Atmos. Chem. Phys. Discuss., doi:10.5194/acp-2016-570, 2016
Manuscript under review for journal Atmos. Chem. Phys.
Published: 8 July 2016

Atmospheric Chemistry and Physics Discussions

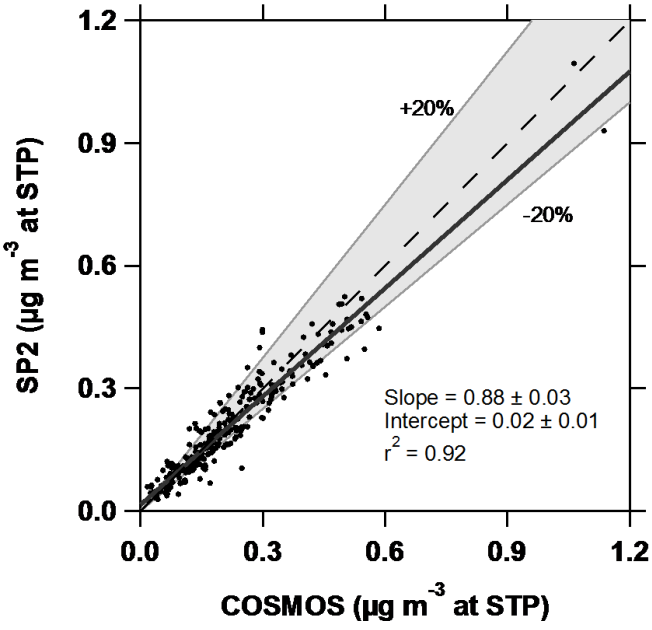

592

593

594 **Figure 2.** Correlation plot of SP2-rBC and COSMOS-EBC mass concentrations (at

595 STP). The shaded region corresponds to within ±20%.

596

Atmos. Chem. Phys. Discuss., doi:10.5194/acp-2016-570, 2016
Manuscript under review for journal Atmos. Chem. Phys.
Published: 8 July 2016

Atmospheric Chemistry and Physics Discussions

597

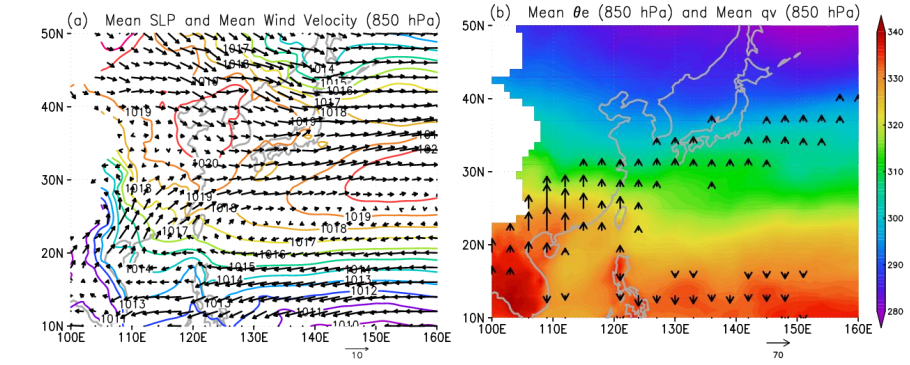

598

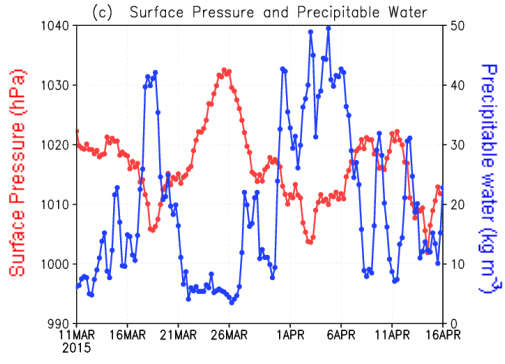

599

600 **Figure 3.** Meteorological fields in East Asia during the observation period (March
601 11-April 14, 2015) based on NCEP FNL data. (a) Mean SLP (hPa, contours) and
602 mean horizontal wind velocity at the 850-hPa level (m s^{-1}). Regions without data
603 correspond to those of high-altitude mountains. (b) Mean θe (K) and total meridional
604 moisture transport (qv values) at the 850-hPa level (m s^{-1} g kg^{-1}). Only qv vectors
605 with magnitudes greater than 10 m s^{-1} g kg^{-1} were plotted. (c) Temporal variations in
606 the surface pressure (hPa, red line and markers with left axis) and precipitable water
607 (kg m^{-2}, blue line and markers with right axis) at the Fukue observation site (32.75°N,
608 128.68°E).

609

Atmos. Chem. Phys. Discuss., doi:10.5194/acp-2016-570, 2016
Manuscript under review for journal Atmos. Chem. Phys.
Published: 8 July 2016

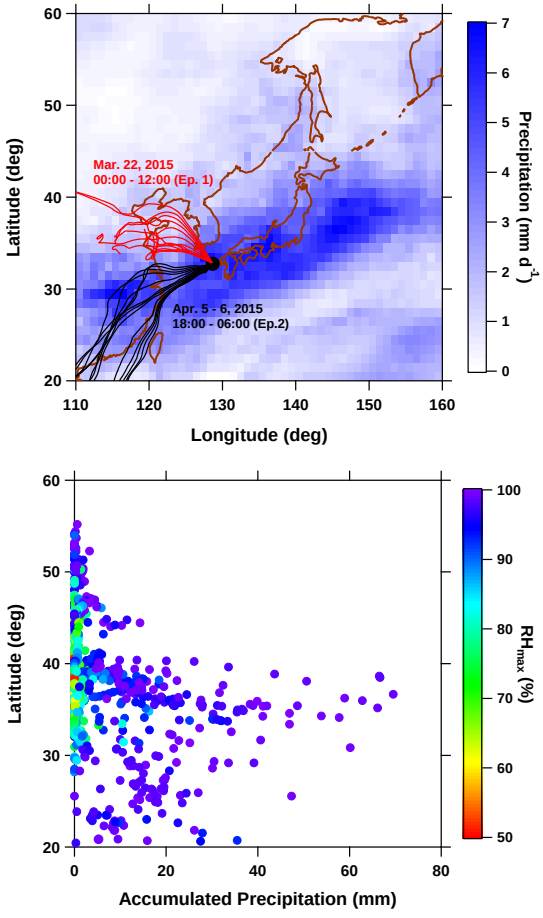

Figure 4. (a) Mean precipitation derived from GPCP during the observation period (March 11-April 14, 2015). 3-day backward trajectories for selected periods are overlaid (Red lines, 00:00-12:00LT March 22, 2015 (Ep.1); Black lines, 08:00LT April 5-06:00LT April 6, 2015 (Ep.2)). (b) The relationship between APT and Lat_{ORIG} (see text for details) colored by the maximum RH along the backward trajectories.

Atmos. Chem. Phys. Discuss., doi:10.5194/acp-2016-570, 2016
Manuscript under review for journal Atmos. Chem. Phys.
Published: 8 July 2016

Atmospheric Chemistry and Physics Discussions

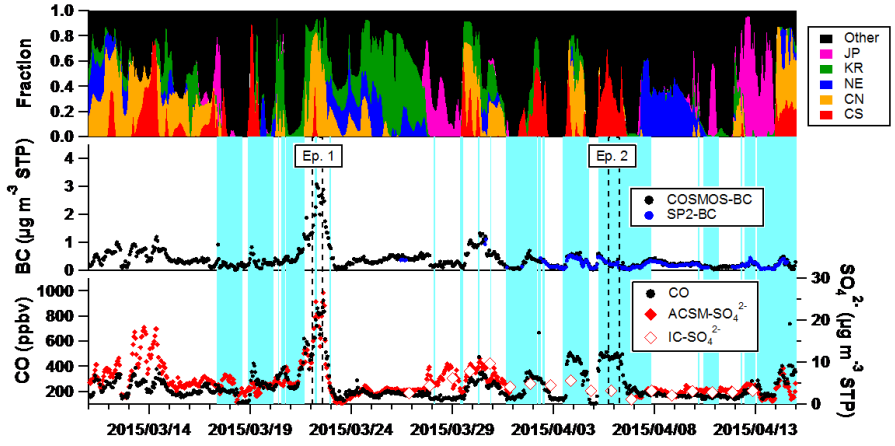

619

620 **Figure 5.** Temporal variations in air mass origin and concentration of trace species.
621 (Top panel) Fractional residence time of air masses passed over selected area (Red,
622 Central South China; Orange, Central North China; Blue, Northeast China; Green,
623 Korea; Pink, Japan; Black, other regions such as Ocean). (Middle panel) mass
624 concentrations of BC measured using the COSMOS (black markers) and SP2 (blue
625 markers). (Bottom panel) concentrations of CO (black markers) and SO_4^{2-} (red
626 circles and open diamond for ACSM and IC, respectively). The periods with the APT
627 > 3 mm are highlighted in light blue in the middle and bottom panels. The periods
628 denoted as Ep.1 and Ep.2 (see the text for details) were enclosed by dashed lines.

629

Atmos. Chem. Phys. Discuss., doi:10.5194/acp-2016-570, 2016
Manuscript under review for journal Atmos. Chem. Phys.
Published: 8 July 2016

Atmospheric Chemistry and Physics Discussions

630

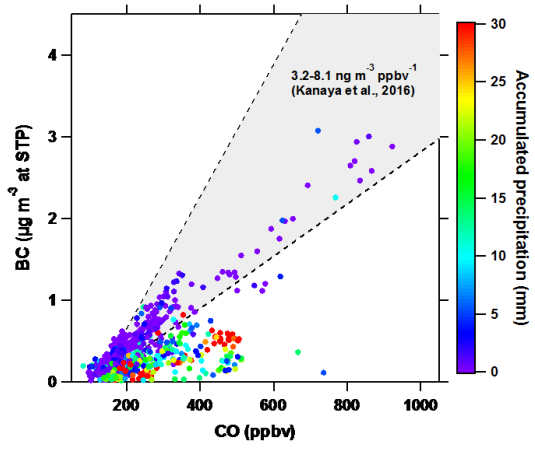

631

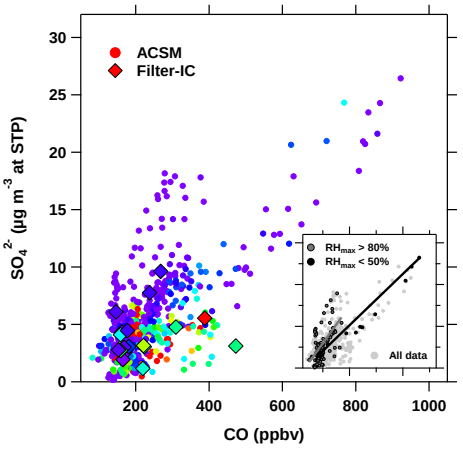

632

633 **Figure 6.** Correlation between aerosol mass concentrations and CO mixing ratio
634 colored according to the APT. (a) BC measured by COSMOS and (b) SO_4^{2-} measured
635 by ACSM and IC (circles and diamond markers, respectively). ACSM- SO_4^{2-}/CO
636 correlations for the zero-APT air masses (no precipitation during transport) with RH
637 greater than 80% (dark shaded markers) or less than 50% (black) are in the subset of
638 6b.

639

Atmos. Chem. Phys. Discuss., doi:10.5194/acp-2016-570, 2016
Manuscript under review for journal Atmos. Chem. Phys.
Published: 8 July 2016

Atmospheric Chemistry and Physics Discussions

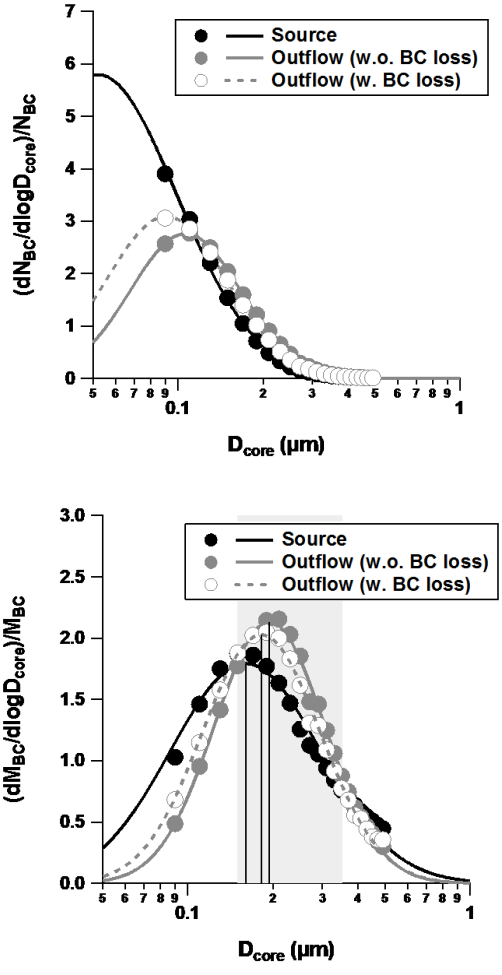

Figure 7. The (a) number and (b) mass size distributions of BC measured at Yokosuka (black markers) and at Fukue Island (gray markers). All the size distributions are normalized by the number or mass concentrations of BC integrated for the diameter range of 0.08-0.5 μm. The size distributions at Fukue Island include the data for the outflow air masses with (open markers) and without (closed markers) BC loss. Lines are the lognormal fitting results. The shaded band in 6(b) corresponds to the size

Atmos. Chem. Phys. Discuss., doi:10.5194/acp-2016-570, 2016
Manuscript under review for journal Atmos. Chem. Phys.
Published: 8 July 2016

Atmospheric Chemistry and Physics Discussions

649 range analyzed to estimate D_s/D_{core} ratios. Vertical lines in 6(b) represent the peak
650 diameter of the lognormal fit for each of three mass size distributions. Note that the
651 peak diameter of Log-normal fit for the BC number size distributions at Yokosuka was
652 estimated from the peak diameter of its mass size distribution (**Table 1**).

Atmos. Chem. Phys. Discuss., doi:10.5194/acp-2016-570, 2016
Manuscript under review for journal Atmos. Chem. Phys.
Published: 8 July 2016

Atmospheric Chemistry and Physics Discussions

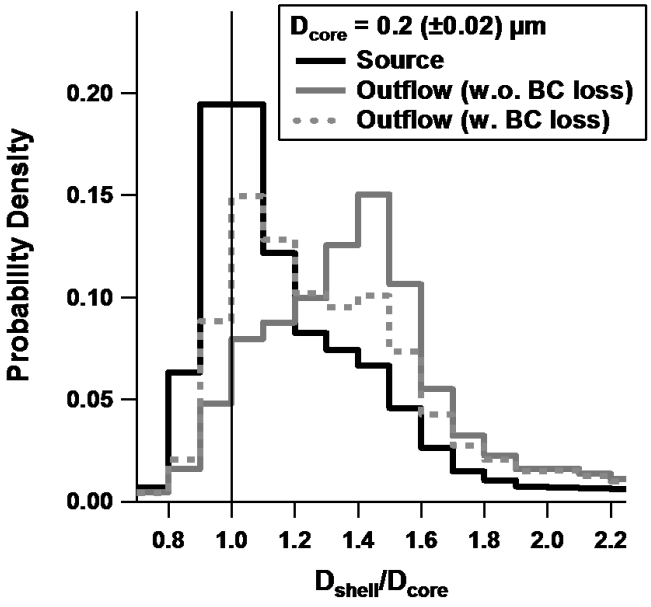

653
654

655 **Figure 8.** Probability density function of the estimated D_s/D_{core} ratios for
656 BC-containing particles with the size 0.2 (±0.02) µm at Yokosuka (Black line) and in
657 air masses of continental outflow with (gray dashed line) and without (gray solid line)
658 BC loss.
659

Atmos. Chem. Phys. Discuss., doi:10.5194/acp-2016-570, 2016
Manuscript under review for journal Atmos. Chem. Phys.
Published: 8 July 2016

Tables

Table 1. Summaries of BC microphysical parameters measured at Yokosuka and Fukue Island

Site	Air mass type	Averaging time*	ΔBC/ΔCO	APT	Log Normal Fit Parameters Avg. (1σ)		1-hr Median D_S/D_{core} for selected D_{core} Avg. (1σ)			
		(hrs)	(ng m^{-3} ppb^{-1})	(mm)	MMD (μm)	σ_g	0.15 - 0.2	0.2 - 0.25	0.25 - 0.3	0.3 - 0.35 (μm)
Yokosuka	Source	184	-	-	0.160 (0.019)	1.84 (0.08)	1.18 (0.07)	1.15 (0.06)	1.10 (0.04)	1.07 (0.04)
Fukue	Outflow	87	>3	1.2	0.195 (0.005)	1.57 (0.05)	1.37 (0.05)	1.32 (0.03)	1.21 (0.03)	1.17 (0.03)
Fukue	Outflow	51	<1	19.9	0.182 (0.011)	1.62 (0.09)	1.25 (0.05)	1.24 (0.04)	1.16 (0.02)	1.12 (0.03)

*Time used for calculating averaged statistics of the microphysical properties of BC-containing particles.